Hindawi
Advances in Polymer Technology
Volume 2020, Article ID 3971953, 9 pages
https://doi.org/10.1155/2020/3971953

Research Article

Colloidal Probes of PNIPAM-Grafted SiO_2 in Studying the Microrheology of Thermally Sensitive Microgel Suspensions

Jing Shang,[1] Ruonan Gao,[1] Fu Su,[1] Huaguang Wang,[2] and Dan Zhu[1]

[1]*Jiangsu Key Laboratory of Bio-functional Materials, College of Chemistry and Material Science, Nanjing Normal University, Nanjing 210023, China*
[2]*Center for Soft Condensed Matter & Interdisciplinary Research, College of Chemistry, Chemical Engineering and Materials Science, Suchow University, Suzhou 215006, China*

Correspondence should be addressed to Huaguang Wang; hgwang@suda.edu.cn and Dan Zhu; zhudan1013@gmail.com

Received 22 August 2019; Revised 1 December 2019; Accepted 13 December 2019; Published 13 January 2020

Academic Editor: Surendar R. Venna

The complex rheology and the phase behavior of thermally sensitive poly(*N*-isopropylacrylamide) (PNIPAM) microgels have been investigated in both the swollen and collapsed states by using microrheology. To avoid the interactions between the tracer probes and the PNIPAM microgels, such as the adsorption or the depletion effect, the probes of silica (SiO_2) particles have been grafted with PNIPAM chains (SiO_2-PNIPAM) and characterized with Fourier transform infrared spectroscopy (FTIR). The successful preparation of SiO_2-PNIPAM has also been proved by the investigation of the particle size and morphology with dynamic light scattering (DLS) and transmission electron microscope (TEM) below and beyond the phase transition temperature of PNIPAM. The microrheology of the PNIPAM microgel suspension has been investigated by using the prepared SiO_2-PNIPAM particles as microrheological probes, and the results show that the diffusive coefficient of the probes in the swollen state is one-fifth of that in the collapsed state, and the viscosity of the PNIPAM microgel suspension in the swollen state is four times higher than that in the collapsed state, indicating SiO_2-PNIPAM is a good probe in the microrheological study of PNIPAM microgel suspensions.

1. Introduction

Colloidal suspensions are defined as fluids with colloidal particles sized approximately between one nanometer and one micrometer dispersed in them. The colloidal suspensions possess specific properties in physiochemistry and transport [1–3]. On the one hand, the colloidal suspensions are commonly used in our daily life and in a diversity of areas of industrial manufacturing, such as coating, cosmetics, and food [4, 5]. On the other hand, they are constantly important in basic research, acting as an ideal model in studying the equilibrium or near-equilibrium phenomena in atomic or molecular physics [6] since the colloidal particles are large enough that the microscopic movements or interactions can be detected by experimental apparatus, and they are small enough as well so that they can be thermally activated and the phase behaviors and dynamics can be related to the sizes, the shapes, the softness, and the Zeta potential of the particles. Both experimental and theoretical research studies are mostly focused on the phase behaviors, crystal formation, glass transition, and viscosity or transport of these ideal models of colloidal suspensions [7–11].

Usually, in the experimental study of those phase behaviors, a series of suspensions of different mass concentrations are prepared, and the physical properties of the bulk system are investigated. However, the state of the particles in the concentrated suspension is deeply affected by the initial conditions and the preparation, which makes the results unrepeatable to some extent. Among various colloidal particles, poly (*N*-isopropylacrylamide) (PNIPAM) microgel particles have attracted great attention because they undergo a volume transition around a critical transition temperature (T_c) of ~32°C [12–14]. The microgels are highly swollen below T_c due to the hydration of PNIPAM, while they are

considerably shrunken above T_c due to dehydration. Therefore, the volume fraction of the microgel particles in the suspension can be adjusted without changing the mass concentration of the particles. This leads to the suspension of PNIPAM microgels acting as a good model system to study the mechanism of phase transitions, especially those close to the critical point, such as gelation or jamming transitions [8, 11].

Meanwhile, it has been reported that the interactions between PNIPAM microgels change from repulsive to attractive when the temperature is higher than T_c. Hence, both the volume and the interactions of the PNIPAM microgels could be modulated by the temperature [15]. In addition, if the suspension is semidilute and above the volume phase transition of T_c, the aggregate of shrunken microgels might lead to both spatially and temporally heterogeneity in the system, which brings a challenge in choosing proper measurements to study the dynamics of PNIPAM microgel suspensions [16].

The conventional measurement method of rheology is to apply a relatively high stress which may lead to a macroscopic deformation and sometimes could destroy structures of the tested samples, e.g., in the case of soft gels or fragile glasses. Therefore, the obtained rheological information is distorted, or some structural details are lost due to the bulk strain responses. Compared with the conventional measurement of rheology, microrheology is to use micrometer-sized particles, termed as tracers or probes, in the system of complex fluid [17–20], either by detecting the Brownian motion of the trajectory of the probes or by actively manipulating them with external forces such as magnetic or electric field, and the local rheology of the complex fluid can be studied. The former is called a passive technique, while the latter is called an active technique. Active measurements allow the possibility of applying large stresses and sometimes large beyond the linear regime to stiff materials in order to obtain detectable strains, which may lead to local deformations of the sample and deformed viscoelastic response [21, 22]. Unlike the active technology, the passive measurements use the thermal energy of probe particles to measure the rheological properties of the tested system [23–26]. The system should be sufficiently soft for those embedded probes to achieve thermally activated movements. The passive particle tracing technique is usually used in detecting the local physical environment in the heterogeneous complex fluids, such as polymeric materials, biological systems, improving our understanding of regional and integrated properties, structures, and transport in live cells.

Microrheology seems a good tool in exploring such heterogeneity with a local modulus and viscosity, characterizing the statistical interactions among the probes and PNIPAM microgels, and thus, the structural heterogeneity of PNIPAM microgel suspension through the volume phase transition can be understood [16]. However, single particle microrheology of the probe does not always possess a good consistency with bulk rheology, and it fails in the study of rheological properties when there are some particular interactions between the probes and the tested system, such as the adsorption of polymers or particles onto the probe surface and the electrostatic or the hydrodynamic interactions [27, 28]. Such interactions between the probes and the tested system are categorized in Figure 1: (a) the microgels are adsorbed onto the probes so that they could form clustering (or gelation) through the microgel bridge and (b) the depletion of the polymer or the microgel could drive the probe particle aggregate.

Therefore, in order to detect the microrheology behaviors of PNIPAM microgel suspension, the tracer probe should be a pseudo-PNIPAM particle, i.e., the probe surface may be grafted with a layer of PNIPAM which behaves like those PNIPAM microgels in the suspension. To this purpose, we have synthesized silica (SiO_2) particle with uniform diameter via Stöber's route [29, 30] and grafted PNIPAM chains on the surface of them via atomic transfer radical polymerization (ATRP) [31]. We use FTIR to characterize the surface chemistry and use tunneling electron microscopy (TEM) and dynamic laser light scattering (DLS) to identify the size and morphology of the SiO_2 particle before and after grafting. They confirm that PNIPAM has been grafted onto the probe particles. We therefore have introduced the grafted particles as tracers to investigate the microrheological property of the PNIPAM suspensions.

2. Experimental Section

2.1. Materials. Tetraethyl orthosilicate (TEOS), triethanolamine (TEA), pyridine, and toluene are analytical reagents purchased from Sinopharm Chemical Reagent Co., Ltd. Toluene is firstly washed with concentrated sulfuric acid to remove impurities such as thiophene and then washed with aqueous solution of sodium bicarbonate and distilled water. After dried with anhydrous magnesium sulfate, toluene is distilled under reduced pressure. 3-Aminopropyl trimethoxysilane, 2-bromoisobutyryl bromide, and *N*,*N*,*N*′,*N*′,*N*″-pentamethyldiethylenetriamine (PMDETA) are from Aladdin and are used as received. Copper(I) bromide (CuBr, Aladdin, 98%) is washed with glacial acetic acid to remove soluble oxidized species, filtrated, washed with ethanol, and dried under vacuum. *N*-isopropylacrylamide (NIPAM, Aladdin, 98%) is recrystallized from the mixture solvent of hexane and benzene with the volume ratio of 6 : 4. *N*,*N*′-methylenebisacrylamide (BIS, Aldrich), sodium dodecyl sulfate (SDS, Aldrich), potassium persulfate (KPS, Aldrich), and other analytic grade reagents are used as received.

2.2. Synthesis of SiO_2 Nanoparticles. Aqueous solution of ammonium (25%, 25 mL) and dehydrate ethanol (500 mL) are put in a three-necked flask and mixed together at room temperature. TEOS (12.5 mL) and dehydrate ethanol (14 mL) are mixed together and added dropwise into the former mixture at the speed of 1 mL/min. The final concentrations of NH_3, water, and TEOS in the mixture are 0.6, 1.7, and 0.1 M, respectively. After reacting at the room temperature for 20 hrs, the suspension is centrifuged at the speed of 8000 rpm and the nanosized SiO_2 particles are obtained. They are further washed with dehydrate ethanol

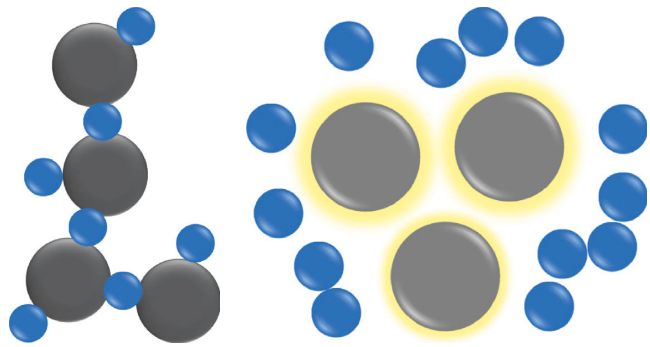

Figure 1: The schematics of the colloidal probes of microrheology (grey spheres) aggregate through (a) bridging, and (b) depletion of the microgels (blue spheres).

and centrifuged three times and fully dried at vacuum at 120°C for 12 hrs. The grafting procedure of PNIPAM chain onto the prepared SiO_2 is schematically described in Figure 2, including the respective introductions of the amine group and the initiator on the surface of SiO_2, and then the PNIPAM grafted from where the acting sites have been introduced.

2.3. Amine Group Fixed on the Surface of SiO_2. 1.00 g SiO_2, 0.1 mL TEOS, and 50 mL dehydrate ethanol are put in the flask and fully dispersed under ultrasonic treatment. The liquid is heated to 60°C, and then a mixture of 60 μL aqueous solution of ammonium, 1.5 mL deionized water, and 0.94 mL APS are added dropwise. The reaction is maintained at 50°C for 12 hrs, then cooled to room temperature, centrifuged at 8000 rpm, and washed by ethanol three times to remove the unreacted APS. The amine-functionalized SiO_2 is obtained and dispersed in toluene before usage.

2.4. Initiator Fixed on the Surface of SiO_2. 0.4 mL pyridine is added into the suspensions of amine-functionalized SiO_2, at the temperature of 0°C, 0.5 mL 2-bromoisobutyryl bromide (BIBB) is added, and the reaction continues at 0°C for 1 h and then at room temperature for 24 hrs. After centrifuged and washed with ethanol for three times, the obtained SiO_2 with initiator fixed on the surface is dried at vacuum at 80°C for 24 hrs.

2.5. PNIPAM Grafted from the Surface of SiO_2. The obtained initiator-fixed SiO_2 (400 mg) and PMDETA (78 μL) are put in 8 mL deionized water, after ultrasonically dispersed into uniform suspension, it is poured into the Schlenk bottle, and three cycles of freezing-thawing are carried out to remove the oxygen. In the state of frozen and with nitrogen protection, 50 mg CuBr is added, and after two cycles of freezing-thawing and stirring, the reaction continues at room temperature for 1 h. The NIPAM is polymerized from the surface of SiO_2. The grafted particles are obtained after washed with deionized water and centrifuged three times. The products are noted as SiO_2-PNIPAM.

2.6. Preparation of PNIPAM Microgel. The relatively homogeneously crosslinked microgels of PNIPAM are prepared by precipitation polymerization at 70°C in water. The purified monomer of NIPAM (1.613 g), the cross-linker of BIS (0.07 g), and surfactant of SDS (0.034 g) are dissolved in 140 mL of deionized water in a 250 ml three-necked flask with a reflux condenser, put in an oil bath of 40°C, and stirred with a magnetic stirring. After nitrogen gas is purged for 1.5 hrs, KPS (0.09 g) is dissolved in 10 ml deionized water and is fed with an injection syringe. The temperature is gradually raised to 70°C, and another BIS (0.02 g) is dissolved in 5 mL deionized water and is fed by a syringe pump at the rate of 20 ml/h. The reaction is continued at a temperature of 70°C for 4 hrs. The details of the polymerization of NIPAM into linear chains with narrowly distributed molecular weight or gel networks have been described elsewhere [13, 32]. The characterizations of the microgels' structure and thermally responsive behavior are shown in the Supplementary Materials (available here).

2.7. Characterizations. Zetasizer Nano ZS90 from Malvern, UK, with a 10 mW and 635 nm laser and the scattering angle of 90° is used to estimate the hydrodynamic size distribution and the Zeta potential of the synthesized SiO_2 and the grafted SiO_2-PNIPAM nanoparticles. The temperature is controlled in the range of 5–50°C by a thermostat, so that the temperature dependence of the size and the Zeta potential of the studied particles can be evaluated. The SiO_2 and SiO_2-PNIPAM are ground with KBr and studied with an FTIR spectrometer, Tensor 27 from Bruker, Germany. By attributing the absorptions in the range from 400 cm^{-1} to 40000 cm^{-1}, the chemical structures of the particles can be obtained so that the grafting of PNIPAM can be verified. Thermogravimetric analysis (TGA) is performed by using the STA449F3 analyzer, Netzsch, Germany, from the temperature range from 25°C to 800°C. 5–10 mg specimens were heated at the atmosphere of nitrogen and at the heating rate of 10°C/min. By detecting the mass difference before and after heating at the temperature of the fuse point of organic materials, the amount of the PNIPAM grafted onto the SiO_2 surface can be deduced. Transmission electron microscope (TEM), H-7650 from HITACHI, Japan, is used to identify

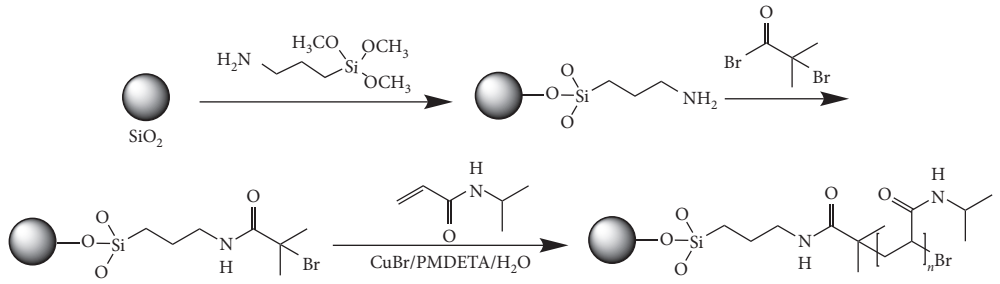

Figure 2: The schematics of the grafting procedure of PNIPAM on SiO_2.

the particle size and morphology. The specimen is ultrasonically dispersed in ethanol and dropped onto a copper mesh, and the observation is performed after the solvent is evaporated.

2.8. Principles and Measurements of Particle Tracking Passive Microrheology. The SiO_2-PNIPAM particles are used as tracers and suspended with a concentration of 0.8 wt.% into the PNIPAM hydrogel dispersions (3.0 wt.%). The PNIPAM microgel suspension, together with SiO_2-PNIPAM probes, has been dipped onto the glass plate and sealed with glue and confined to a quasi-2D chamber between two glass coverslips (Fisher). The inverse microscope used is Axio Observer. Video microscopy is used to record the image data for 120 seconds at a rate of 10 frames per second by using a CCD camera, Sony. The magnitude is 1000 times, and the pixels in the field of view are 1392×1040. The area of the view is $134 \times 100\,\mu m^2$ with the pixel size of $0.096\,\mu m$/pixel, and a number of 4800 probe particles have been imaged, and their trajectory has been analyzed with the program of Interactive Data Language (IDL) [33]. Normally, IDL can determine the position of each probe by its center of mass in each image, as well as their position change with time.

Micron-sized spheres in a purely viscous medium undergo simple diffusion or Brownian motion. The dynamics of particle motions are revealed in the time-dependent position correlation function of individual tracers. This correlation function, also known as the mean-squared displacement (MSD), is defined as the deviation of the position of a particle with respect to a reference position over time, namely,

$$\mathrm{MSD} \stackrel{\mathrm{def}}{=} \left\langle \Delta r^2(\tau) \right\rangle = \left\langle |r(t+\tau) - r(t)|^2 \right\rangle, \quad (1)$$

where $r(t)$ is the reference position of each particle and $r(t+\tau)$ is the position of each particle in a determined time.

In a complex system exhibiting both viscous and elastic behavior, the responses are typically frequency-dependent and depend on the time and length scale probed by the measurement. The mean-squared displacement of the probe particles is recorded and related to the macroscopic linear viscoelastic moduli of the system by using a generalized Stokes–Einstein relationship. On assuming that the probes embedded present sublinear integration-time dependence, the system is of viscoelastic properties obtaining a complex viscoelastic modulus, which is termed in the following equation:

$$G^*(\omega) = G'(\omega) + iG''(\omega), \quad (2)$$

where $G'(\omega)$ is the elastic (conservative) part and $G''(\omega)$ is the viscous (dissipative) part, and ω is the angular frequency of the pulsation. The generalized Stokes–Einstein relationship is expressed in the following equation:

$$\left\langle \widetilde{G}(s) \right\rangle = \frac{k_B T}{\pi a s \left\langle \Delta \widetilde{r}^2 \right\rangle}, \quad (3)$$

where $\widetilde{G}(s)$ is the Laplace transform of G^*, s is the Laplace frequency, $\Delta\widetilde{r}^2$ is the Laplace transform of the MSD, k_B is the Boltzmann constant, T is the temperature in Kelvin, and a is the radius of the probe particle. Equation (3) provides the relation between the thermal energy density of a particle with the radius of a and the elastic energy needed to deform a material with a complex modulus of G^*.

3. Results and Discussion

The FTIR spectra of SiO_2, initiator-modified SiO_2, and PNIPAM-grafted SiO_2 are shown in Figure 3. In Figure 3(a) for SiO_2, the absorption bands observed at $1100\,cm^{-1}$ and $815\,cm^{-1}$ attribute to the asymmetric stretching vibration of Si-O-Si, while that at $470\,cm^{-1}$ is assigned to its bending vibration. In Figure 3(b), for the modified SiO_2-BIBB, the strong absorption at $1635\,cm^{-1}$ attributes to the C=O stretching of BIBB, and those at $1390\,cm^{-1}$ and $946\,cm^{-1}$ are from the symmetric deformation and wagging vibrations of methyl, indicating that the initiator has been successfully introduced onto the surface of SiO_2. In Figure 3(c), for SiO_2-PNIPAM, two bands at $1647\,cm^{-1}$ and $1541\,cm^{-1}$ are the typical signals of amides, Band I is assigned to the stretching vibration of C=O and Band II to the bending of N-H and stretching of C-N [34, 35]. Bands at $1463\,cm^{-1}$ and $1398\,cm^{-1}$ are assigned to the -$CH(CH_3)_2$ vibrational absorption, and band at $1172\,cm^{-1}$ is from the skeletal stretching vibration of C-C in the group of -$CH(CH_3)_2$. The above analysis indicates that PNIPAM has been successfully grafted onto the SiO_2.

The grafting amount of PNIPAM onto SiO_2 can be quantitatively deduced from the TGA analysis in Figure 4. The thermal decomposition of SiO_2, initiator-modified SiO_2, and PNIPAM-grafted SiO_2 occurs when the temperature is from 25°C to 800°C.

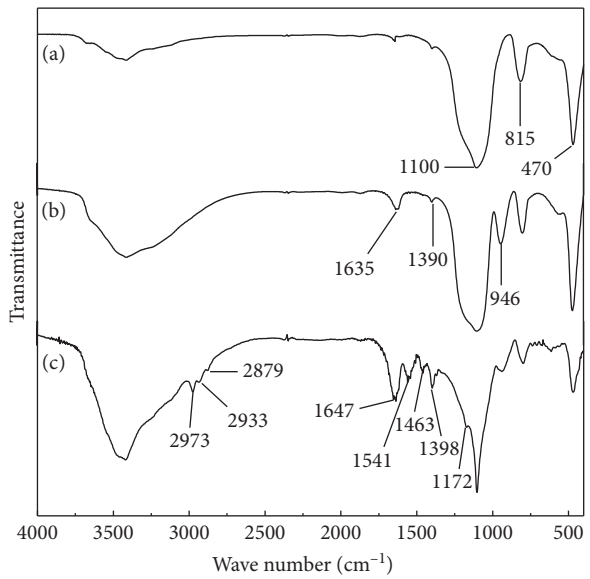

Figure 3: The FTIR spectra of (a) SiO_2, (b) SiO_2-BIBB, and (c) SiO_2-PNIPAM.

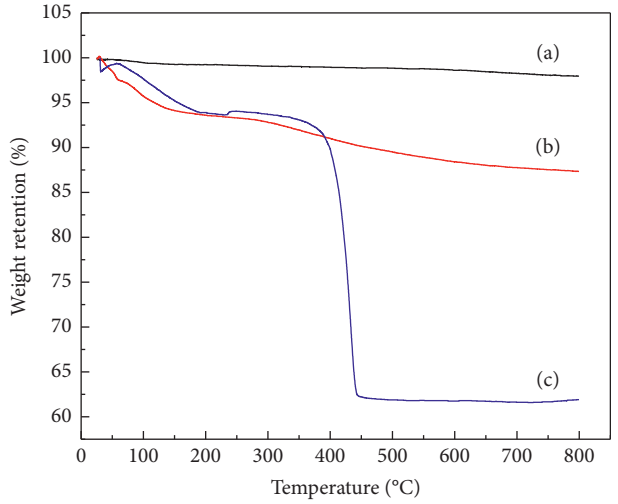

Figure 4: TGA curves of (a) SiO_2, (b) SiO_2-BIBB, and (c) SiO_2-PNIPAM.

The nanoparticle of SiO_2 shows retention about 97.9%, while that of SiO_2-BIBB and SiO_2-PNIPAM is 87.3% and 61.9%, respectively. The weight loss of SiO_2-PNIPAM is obviously higher than that of SiO_2 and SiO_2-BIBB, due to the decomposition and removal of PNIPAM. It indicates that the PNIPAM has been successfully grafted onto the SiO_2. From the TGA data, the grafting degree of PNIPAM, G_y, can be deduced from equation (4). W_{PNIPAM} is the mass difference between SiO_2-PNIPAM and SiO_2-BIBB, and the result is 25.4 wt.%, meaning that for 1 g SiO_2, 0.25 g PNIAPM can be grafted onto the surface:

$$G_y(\%) = \frac{W_{PNIPAM}}{W_{SiO_2}} \times 100. \quad (4)$$

Figure 5 shows the size and morphology of the nanoparticle of SiO_2 before and after PNIPAM grafting observed with TEM, with the amplification of 20,000 times. The spheres in the view are uniform in size, and there is a pale-colored shadow around the particle for SiO_2-PNIPAM, which might attribute to the organic substance. The distinct morphology difference between SiO_2 and SiO_2-PNIPAM further provides an indication that the PNIAPM is grafted onto the SiO_2 particles.

Figure 6 shows the size distribution measured by the dynamic light scattering. Before grafting, the average size of SiO_2 is 590 nm and PDI is 0.083, while after grafting, the average size is 856 nm and PDI is 0.078. This confirms the grafting of PNIPAM on the SiO_2 particles. The fact that the diameters measured with LLS are larger than those taken from TEM attributes to the different measuring mechanism of the instrument and the samples' states as well. It is the hydrodynamic radius for the particles dispersed in water measured with the dynamic light scattering, while in the TEM the electron scattering angle is decided by the electron density of the dry particles on the copper mesh. Therefore, from Figure 5, it is difficult to distinguish the sizes between SiO_2 and SiO_2-PNIPAM.

Figure 7 shows the average size and the Zeta potential of the SiO_2-PNIPAM in distilled water, measured at various temperatures. When the temperature rises to 32°C, as shown in Figure 7(a), the particle size shrinks abruptly from 840 nm to 720 nm, which is in agreement with the LCST of PNIPAM at 32°C [13, 30]. At 25°C, water is a good solvent for PNIPAM, so that the chains are of coil form and the hydrodynamic radius of the SiO_2-PNIPAM is large, while at the temperature above 32°C, the PNIPAM chains collapse and the radius decreases.

Figure 7(b) shows the Zeta potential of SiO_2-PNIPAM at different temperatures. The absolute value of Zeta potential of SiO_2-PNIPAM increases abruptly at the temperature range of 34–40°C. This is due to the releasing of counterions formerly condensed at the PNIPAM chains. The radius and Zeta potential of the SiO_2-PNIPAM particles change with temperature are all relevant with the phase transition of PNIPAM dependent on temperature [13, 14, 36], indirectly confirming the successful grafting of PNIPAM on the SiO_2 particles.

The relatively homogeneously crosslinked microgels of PNIPAM are prepared and fully dialyzed in deionized water for three weeks before characterizations and microrheology testing. The hydrodynamic size and its distribution of the synthesized PNIPAM microgels are estimated with dynamic laser light scattering, which shows an average size of 120 nm at 25°C and 50 nm above the LCST of PNIPAM. A suspension of microgels with a mass concentration of 3% has been made, and the SiO_2-PNIPAM probes have been added with the concentration of 0.8%. We have used IDL (Interactive Data Language) to detect the probe particles. The typical trajectories of the SiO_2-PNIPAM probes in PNIPAM microgel suspension at two different temperatures are shown in Figure 8. In Figure 8, the pink lines are the trajectory taken for 5 s of the probe particles, center of the

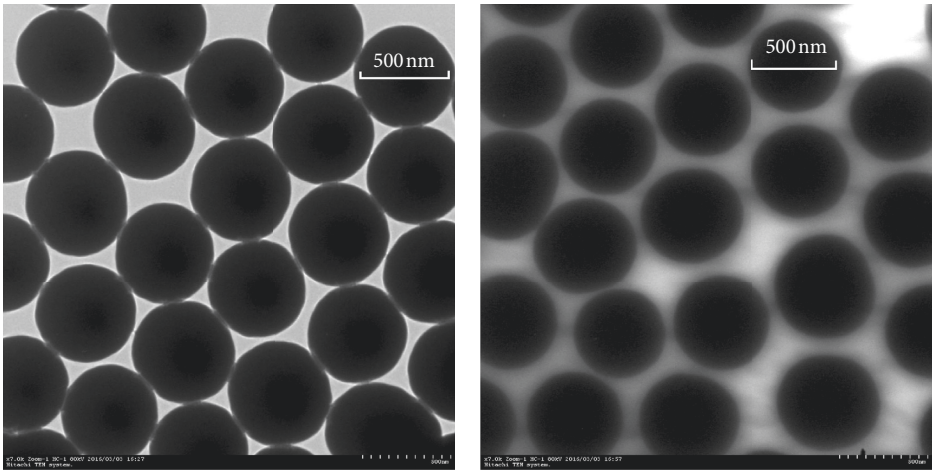

(a) (b)

Figure 5: The TEM images of (a) SiO_2 and (b) SiO_2-PNIPAM.

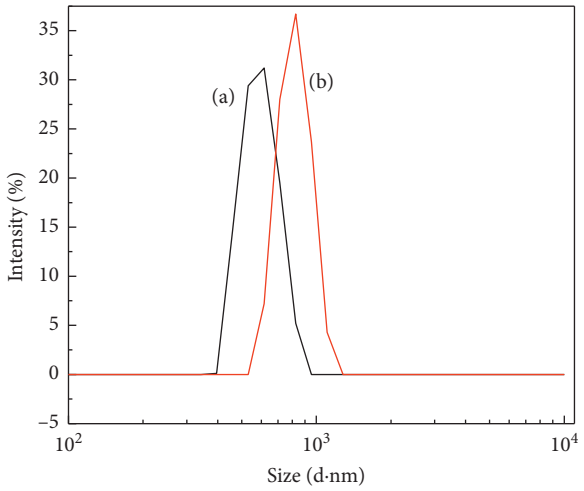

Figure 6: The size distribution of the nanoparticles of (a) SiO_2 and (b) SiO_2-PNIPAM.

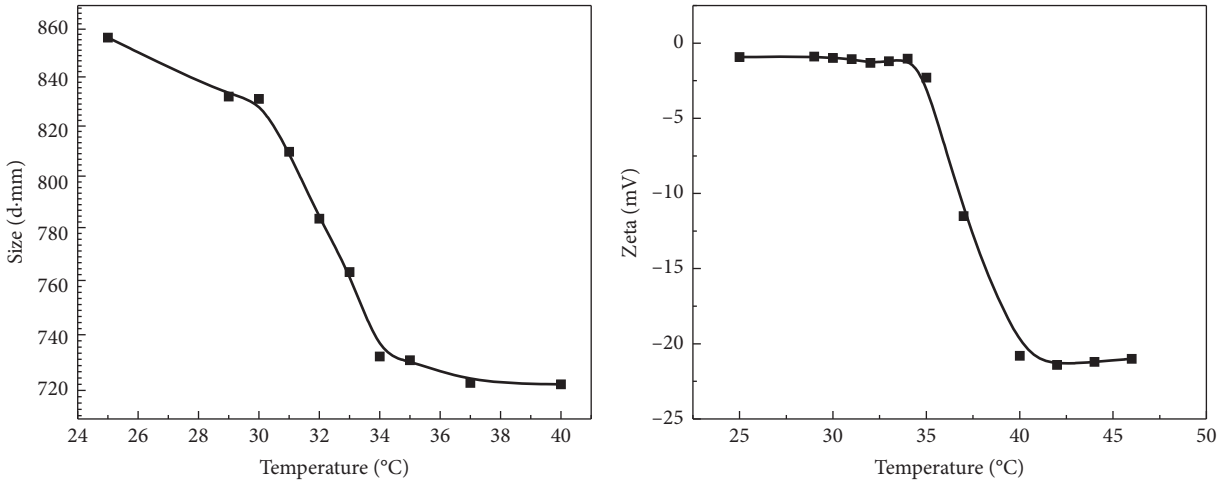

(a) (b)

Figure 7: The temperature-dependent (a) average size and (b) Zeta potential of the SiO_2-PNIPAM particles.

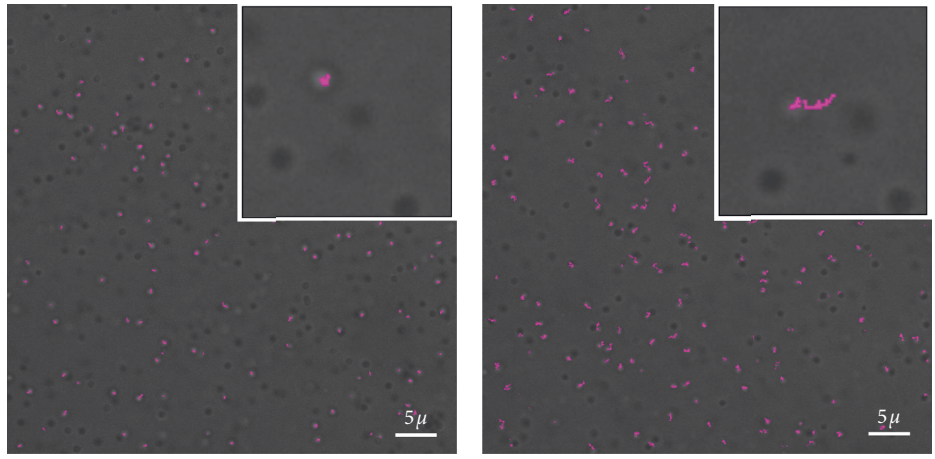

(a) (b)

Figure 8: The trajectory of 5 seconds of the SiO_2-PNIPAM probes in PNIPAM dispersion at (a) 20°C and (b) 32°C. The insets on the top right show the amplified record of the single particle movements.

particles, which are shown on the focal plane, and they are traced and used for statistical calculation, while the dark ones are those out of the plane. Clearly, larger movements of the particles are observed in the high-temperature collapsed state (32°C) of the suspension compared with that in the low-temperature swollen state (20°C).

The MSD can be deduced from the method of directly tracking the particle position as a function of time. The entire particles' trajectories are obtained, allowing further analysis of individual trajectory beyond an ensemble-averaged MSD. The displacement distribution of the probes in PNIPAM suspension is shown in Figure 9, and Gaussian function has been used to fit the distribution.

When particle achieves a free diffusion in a purely viscous material, the corresponding MSD should grow linearly with sampling integration time:

$$\left\langle \Delta x^2 \right\rangle = 2D\Delta t, \tag{5}$$

where $\langle \Delta x^2 \rangle$ is the average displacement square of all the probes and D is the diffusion coefficient. According to the Stokes–Einstein equation,

$$D = \frac{k_B T}{6\pi\eta a}, \tag{6}$$

where k_B is the Boltzmann constant, T is the absolute temperature of the system, η is the viscosity of the system, and a is the radius of the probe particles. We have deduced the diffusive coefficients of the probes of SiO_2-PNIPAM at 20°C and 32°C and the viscosity of PNIPAM suspension at the two temperatures. The results are shown in Table 1, from which the diffusion coefficient of the probes at 20°C is 0.18 $\mu m^2/s$, which is lower than that at 32°C of 0.94 $\mu m^2/s$. The viscosity derived from Stokes–Einstein equation at 20°C is 4.77 mPa·s, much higher than that at 32°C, which is 0.95 mPa·s and close to the viscosity of water at 32°C [37]. Here, the radius of the probe particle we have used is from TEM, which is 250 nm. Theoretically, it is the hydrodynamic radius, which is obtained from the dynamic light scattering

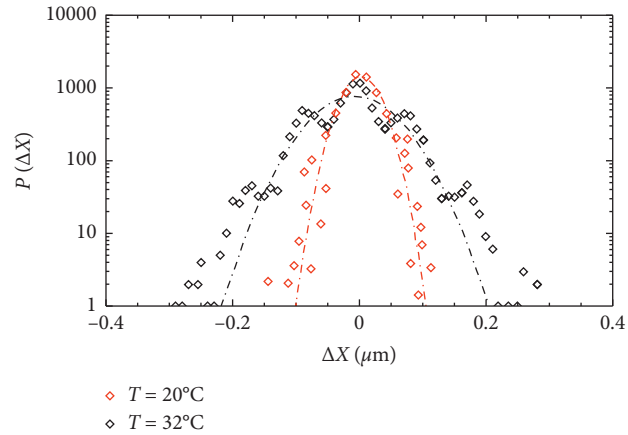

Figure 9: The displacement distribution of the SiO_2-PNIPAM probes in PNIPAM dispersion at 20°C (red) and 32°C (black).

Table 1: The diffusive coefficients of the probes and the viscosity of the medium.

Temperature	D ($\mu m^2/s$)	η (mPa·s)
20°C	0.18	4.77
32°C	0.94	0.95

measurement, shall be used in Stokes–Einstein equation. The particle sizing instrument of Nano ZS90 from Malvern, which measures only at one scattering angle of 90°, is not suitable for polydisperse particles larger than 100 nm, and if there are a few large particles in the suspension, they contribute too much to the scattering intensity so that the measured average size is much larger than the real one. Therefore, we have used the particle size detected by TEM.

As schematically indicated in Figure 10, we draw a physical scenery that when the thermoresponsive microgels shrink, there is more space for the probe particle to move, and thus, the diffusive coefficient of the particle is higher

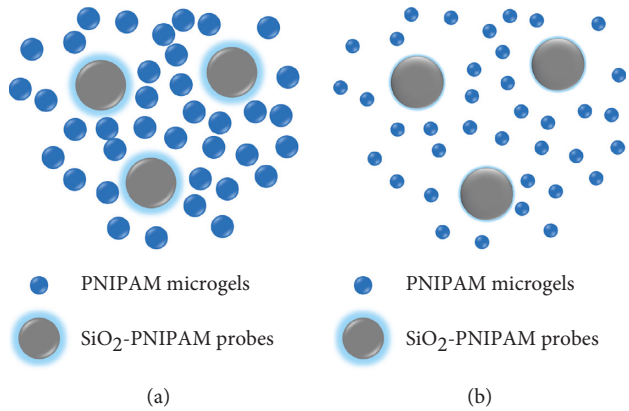

Figure 10: The schematics of the probe particle of SiO_2-PNIPAM (grey) in the water dispersion of PNIPAM microgels (blue) at the temperature of (a) 20°C and (b) 32°C.

and the viscosity of the medium is lower. In previous microrheology studies for PNIPAM suspension, however, the MSD data show that above the phase transition temperature, the tracer particles lose their liquid-like behavior and seem to fall inside a cage [38]. It is assumed that they lose mobility by a restrictive field of depletion forces exerted by the collapsed particles, and we attribute that to the adsorption and bridging of the microgels that make them in the cage of clusters. Therefore, our effort of grafting PNIPAM chains on the tracer particle is necessary to achieve a successful microrheology study of those microgels with soft and attractive surface.

4. Conclusions

The nanoparticles of SiO_2 are synthesized using the Stöber method, and PNIPAM chains are "grafting from" the surface of the SiO_2 by using ATRP. The FTIR is used to characterize the chemical structures of the particles, the DLS and TEM have been used to determine the particle size and morphology, and hydrodynamic radius and Zeta potential have been measured to describe the thermoresponsive behaviors of the grafted particles, and all the above results have confirmed the successful grafting of PNIPAM onto the surface of SiO_2 particles. The grafting density of PNIPAM is obtained by thermogravimetric analysis on a synchronous thermal analyzer. The prepared SiO_2-PNIPAM particles are dispersed into the suspension of PNIPAM microgels as microrheological probes, and the trajectory of the probes is detected and analyzed. The characteristic microrheology of the PNIPAM microgel suspension suggests an obvious change in probes' diffusive coefficient and viscosity below and above the volume phase transition temperature of PNIPAM, suggesting the necessities and advantages of PNIPAM grafted probes in the microrheology study of PNIPAM microgel suspensions.

Data Availability

All data and analyses necessary to understand and assess the conclusions of the manuscript are presented in the main text.

Conflicts of Interest

The authors declare that they have no conflicts of interest.

Acknowledgments

This research has been financially supported by the National Natural Science Foundation of China (51273091, 21204037, and 11704269).

Supplementary Materials

In the supplementary, the synthesis of the thermally sensitive PNIPAM microgels used in the microrheology studies has been described. The characterizations of the microgels' structure, size, and thermally responsive behaviors have been shown. (*Supplementary Materials*)

References

[1] P. J. Lu and D. A. Weitz, "Colloidal particles: crystals, glasses, and gels," *Annual Review of Condensed Matter Physics*, vol. 4, no. 1, pp. 217–233, 2013.

[2] I. D. Morrison and S. Ross, *Colloidal Dispersions: Suspensions, Emulsions, and Foams*, Wiley-Interscience, New York, NY, USA, 2002.

[3] A. Fernandez-Nieves, H. Wyss, J. Mattsson, and D. A. Weitz, *Microgel Suspensions: Fundamentals and Applications*, Wiley-VCH Verlag, Weinheim, Germany, 2011.

[4] C. H. Mai, T. T. Diep, T. T. T. Le, and V. Nguyen, "Advances in colloidal dispersions: a review," *Journal of Dispersion Science and Technology*, 2019.

[5] H. F. Mark, *Encyclopedia of Polymer Science and Technology, Concise*, John Wiley & Sons, Hoboken, NJ, USA, 3rd edition, 2013.

[6] S. Lower, "Colloids and their uses," 2019, https://chem.libretexts.org/.

[7] W. Poon, "PHYSICS: colloids as big atoms," *Science*, vol. 304, no. 5672, pp. 830-831, 2004.

[8] W. C. K. Poon and P. N. Pusey, "Phase transition of spherical colloids," in *Observation, Prediction and Simulation of Phase Transitions in Complex Fluids*, M. Baus, L. F. Rull, and J. P. Ryckaert, Eds., NATO ASI Series (Series C: Mathematical

and Physical Sciences) vol. 460, Springer, Dordrecht, Netherlands, 1995.

[9] H. Yoshida, J. Yamanaka, T. Koga, T. Koga, N. Ise, and T. Hashimoto, "Transitions between ordered and disordered phases and their coexistence in dilute ionic colloidal dispersions," *Langmuir*, vol. 15, no. 8, pp. 2684–2702, 1999.

[10] A. K. Arora and B. V. R. Tata, "Interactions, structural ordering and phase transitions in colloidal dispersions," *Advances in Colloid and Interface Science*, vol. 78, no. 1, pp. 49–97, 1998.

[11] R. T. Bonnecaze and M. Cloitre, "Micromechanics of soft particle glasses," *High Solid Dispersions*, vol. 236, pp. 117–161, 2010.

[12] H. G. Schild, "Poly (N-isopropylacrylamide): experiment, theory and application," *Progress in Polymer Science*, vol. 17, no. 2, pp. 163–249, 1992.

[13] S. Zhou, S. Fan, S. C. F. Au-yeung, and C. Wu, "Light-scattering studies of poly (N-isopropylacrylamide) in tetrahydrofuran and aqueous solution," *Polymer*, vol. 36, no. 7, pp. 1341–1346, 1995.

[14] X. Wang, X. Qiu, and C. Wu, "Comparison of the coil-to-globule and the globule-to-coil transitions of a single poly (N-isopropylacrylamide) homopolymer chain in water," *Macromolecules*, vol. 31, no. 9, pp. 2972–2976, 1998.

[15] J. Brijitta, B. V. R. Tata, and T. Kaliyappan, "Phase behavior of poly (N-isopropylacrylamide) nanogel dispersions: temperature dependent particle size and interactions," *Journal of Nanoscience and Nanotechnology*, vol. 9, no. 9, pp. 5323–5328, 2009.

[16] H. Wang, X. Wu, Z. Zhu, C. S. Liu, and Z. Zhang, "Revisit to phase diagram of poly (N-isopropylacrylamide) microgel suspensions by mechanical spectroscopy," *The Journal of Chemical Physics*, vol. 140, no. 2, Article ID 024908, 2014.

[17] M. L. Gardel, M. T. Valentine, and D. A. Weitz, "Microscale Diagnostic Techniques," in *Microrheology*, K. S. Breuer, Ed., pp. 1–49, Springer, Berlin, Germany, 2005.

[18] T. M. Squires and T. G. Mason, "Fluid mechanics of microrheology," *Annual Review of Fluid Mechanics*, vol. 42, no. 1, pp. 413–438, 2010.

[19] W. Liu and C. Wu, "Rheological study of soft matters: a review of microrheology and microrheometers," *Macromolecular Chemistry and Physics*, vol. 219, no. 3, Article ID 1700307, 2018.

[20] P. Cicuta and A. M. Donald, "Microrheology: a review of the method and applications," *Soft Matter*, vol. 3, no. 12, pp. 1449–1455, 2007.

[21] T. Gisler and D. A. Weitz, "Tracer microrheology in complex fluids," *Current Opinion in Colloid & Interface Science*, vol. 3, no. 6, pp. 586–592, 1998.

[22] M. Weitz, G. M. Gibson, R. M. L. Evans et al., "Measuring storage and loss moduli using optical tweezers: broadband microrheology," *Physical Review E*, vol. 81, no. 2, Article ID 026308, 2010.

[23] T. Paust, *New methods for passive and active microrheology*, Ph.D. thesis, Ulm University, Ulm, Germany, 2012.

[24] E. M. Furst and T. M. Squires, *Microrheology*, Oxford University Press, Oxford, UK, 2017.

[25] R. N. Zia, "Active and passive microrheology: theory and simulation," *Annual Review of Fluid Mechanics*, vol. 50, no. 1, pp. 371–405, 2018.

[26] K.-W. Hsiao, J. Dinic, Y. Ren, V. Sharma, and C. M. Schroeder, "Passive non-linear microrheology for determining extensional viscosity," *Physics of Fluids*, vol. 29, no. 12, Article ID 121603, 2017.

[27] N. M. Kovalchuk and V. M. Starov, "Aggregation in colloidal suspensions: effect of colloidal forces and hydrodynamic interactions," *Advances in Colloid and Interface Science*, vol. 179–182, pp. 99–106, 2012.

[28] J. Luo, G. Yuan, and C. C. Han, "Tuning the bridging attraction between large hard particles by the softness of small microgels," *Soft Matter*, vol. 12, no. 37, pp. 7863–7872, 2016.

[29] W. Stöber, A. Fink, and E. Bohn, "Controlled growth of monodisperse silica spheres in the micron size range," *Journal of Colloid and Interface Science*, vol. 26, no. 1, pp. 62–69, 1968.

[30] G. H. Bogush, M. A. Tracy, and C. F. Zukoski, "Preparation of monodisperse silica particles: control of size and mass fraction," *Journal of Non-crystalline Solids*, vol. 104, no. 1, pp. 95–106, 1988.

[31] Z.-L. Gong, D.-Y. Tang, and Y.-D. Guo, "The fabrication and self-flocculation effect of hybrid TiO_2 nanoparticles grafted with poly (N-isopropylacrylamide) at ambient temperature via surface-initiated atom transfer radical polymerization," *Journal of Materials Chemistry*, vol. 22, no. 33, pp. 16872–16879, 2012.

[32] J. Zhou, J. Wei, T. Ngai, L. Wang, D. Zhu, and J. Shen, "Correlation between dielectric/electric properties and cross-linking/charge density distributions of thermally sensitive spherical PNIPAM microgels," *Macromolecules*, vol. 45, no. 15, pp. 6158–6167, 2012.

[33] J. C. Crocker and E. R. Weeks, "Particle Tracking Using IDL," 1996, http://www.physics.emory.edu/faculty/weeks//idl/micrheo.html.

[34] T. Wu, Y. Zhang, X. Wang, and S. Liu, "Fabrication of hybrid silica nanoparticles densely grafted with thermoresponsive poly (N-isopropylacrylamide) brushes of controlled thickness via surface-initiated atom transfer radical polymerization," *Chemistry of Materials*, vol. 20, no. 1, pp. 101–109, 2008.

[35] Z.-J. Liu, Y.-L. Liang, F.-F. Geng et al., "Preparation of poly (N-isopropylacrylamide) brush grafted silica particles via surface-initiated atom transfer radical polymerization used for aqueous chromatography," *Frontiers of Materials Science*, vol. 6, no. 1, pp. 60–68, 2012.

[36] R. Gui and H. Jin, "Temperature-regulated polymerization and swelling/collapsing/flocculation properties of hybrid nanospheres with magnetic cores and thermo/pH-sensitive nanogel shells," *RSC Advances*, vol. 4, no. 6, pp. 2797–2806, 2014.

[37] https://wiki.anton-paar.com/en/water/.

[38] F. J. Guevara-Pantoja, F. Gómez-Galván, I. E. Cipriano, H. Mercado-Uribe, and J. C. Ruiz-Suárez, "Microrheology and electrical conductivity of a dilute PNIPAM suspension," *Rheologica Acta*, vol. 53, no. 2, pp. 159–164, 2014.